Environmental Science & Technology

pubs.acs.org/est

Article

Natural Analogues in pH Variability and Predictability across the Coastal Pacific Estuaries: Extrapolation of the Increased Oyster Dissolution under Increased pH Amplitude and Low Predictability Related to Ocean Acidification

Nina Bednaršek,* Marcus W. Beck, Greg Pelletier, Scott Lee Applebaum, Richard A. Feely, Robert Butler, Maria Byrne, Betsy Peabody, Jonathan Davis, and Jasna Štrus

Cite This: *Environ. Sci. Technol.* 2022, 56, 9015−9028

Read Online

ACCESS | Metrics & More | Article Recommendations | Supporting Information

ABSTRACT: Coastal-estuarine habitats are rapidly changing due to global climate change, with impacts influenced by the variability of carbonate chemistry conditions. However, our understanding of the responses of ecologically and economically important calcifiers to pH variability and temporal variation is limited, particularly with respect to shell-building processes. We investigated the mechanisms driving biomineralogical and physiological responses in juveniles of introduced (Pacific; *Crassostrea gigas*) and native (Olympia; *Ostrea lurida*) oysters under flow-through experimental conditions over a six-week period that simulate current and future conditions: static control and low pH (8.0 and 7.7); low pH with fluctuating (24-h) amplitude (7.7 ± 0.2 and 7.7 ± 0.5); and high-frequency (12-h) fluctuating (8.0 ± 0.2) treatment. The oysters showed physiological tolerance in vital processes, including calcification, respiration, clearance, and survival. However, shell dissolution significantly increased with larger amplitudes of pH variability compared to static pH conditions, attributable to the longer cumulative exposure to lower pH conditions, with the dissolution threshold of pH 7.7 with 0.2 amplitude. Moreover, the high-frequency treatment triggered significantly greater dissolution, likely because of the oyster's inability to respond to the unpredictable frequency of variations. The experimental findings were extrapolated to provide context for conditions existing in several Pacific coastal estuaries, with time series analyses demonstrating unique signatures of pH predictability and variability in these habitats, indicating potentially benefiting effects on fitness in these habitats. These implications are crucial for evaluating the suitability of coastal habitats for aquaculture, adaptation, and carbon dioxide removal strategies.

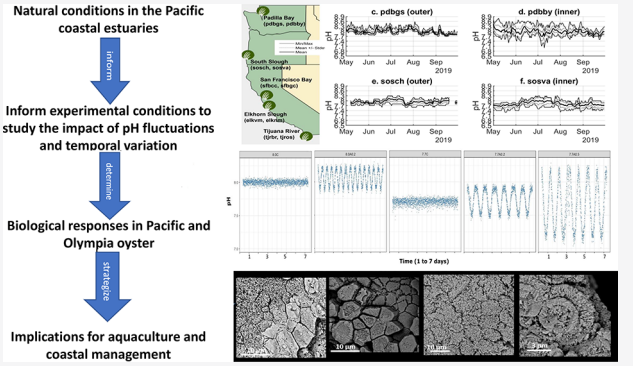

KEYWORDS: *ocean acidification, diel pH variability, amplitude, Crassostrea gigas, Ostrea lurida, shell dissolution, predictability, physiological responses, artificial intelligence automated analyses*

1. INTRODUCTION

Estuaries are one of the most productive regions of coastal ecosystems. In comparison with the open ocean, coastal-estuarine systems are characterized by intense, diel fluctuating carbonate chemistry dynamics that result in heterogeneity in ocean acidification (OA) conditions over spatial and temporal scales. Climate change impacts on coastal estuaries are evident through increasing frequency and magnitude of extreme climate events, ultimately driving the severity of OA exposure.[1−5]

Understanding the components in the carbonate system for which fluctuations have the greatest impact on the most sensitive species' biological responses is critical for managing coastal-estuarine habitats. These habitats provide essential ecosystem services, such as coastal protection processes and nursery grounds for fisheries, and support aquaculture industries that are vital to the livelihoods of millions.[6−8]

Dynamics at the coastal-estuarine interface are modulated by multiple physical−chemical processes, such as photosynthesis, respiration, riverine inputs, sedimentary redox reactions, and tides.[5,9,10] Globally, since preindustrial times, anthropogenic CO_2 input to the ocean has resulted in the intensification of OA, marked by a decline in the ocean pH and carbonate

Received: January 2, 2022
Revised: April 19, 2022
Accepted: April 20, 2022
Published: May 12, 2022

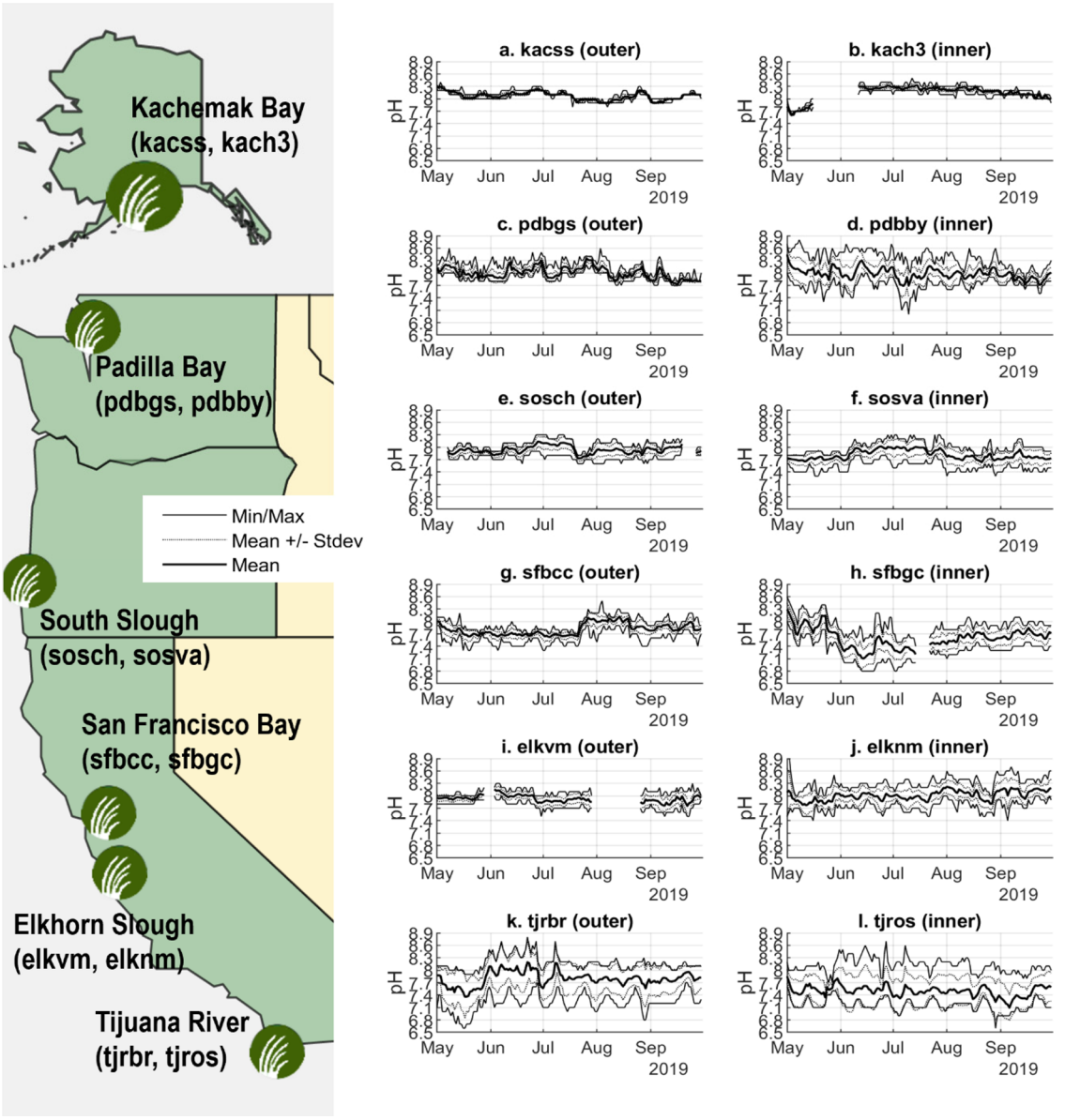

Figure 1. Diel pH mean conditions (heavy solid lines), mean ± diel stdev (dotted lines), and diel pH range (thin solid lines) from across various estuaries along the Pacific coast [(a), (b) Kachemak Bay (AK), (c), (d) Padilla Bay (WA); (e), (f) South Slough (OR); (g), (h) San Francisco Bay (CA); (i), (j) Elkhorn Slough (CA); (k), (l) Tijuana River (CA)] on the outer (seaward, shown in the right panels b, d, f, h, j, l) and inner (landward, away from the ocean, shown in the center panels a, c, e, g, i, k) sides, with the map depicting the locations (left panel). Data range from May to September 2019, coinciding with juvenile oyster presence in these habitats.

saturation state (Ω) (refs 5, 11, 12, and references therein). Although predictions of future variability in estuarine acidification are sparse, climate change-driven alterations in estuarine carbonate diel dynamics result in increased amplitude of variation and pH extremes because of decreasing buffering capacity.[3−5,13−18] One of the important components of the spatial and temporal variability at the coastal-estuarine interface is also the "predictability" pattern (i.e., temporal variation or cyclicity with differing regularity of pH conditions), the term indicating the extent to which the current environmental states allow an organism to effectively predict future states.[19−22] More predicable habitats allow organisms to track and anticipate the conditions and adjust their responses through external, cue-based feedforward mechanisms[23] more accurately. A consensus from the theory of evolution in fluctuating environments is that plasticity (i.e., the ability of a single genotype to alter its phenotype in response to a change in environmental conditions) is favored in environments that fluctuate predictably.[19,21,23,24] As such, the variability of coastal pH conditions (i.e., predictability of environmental changes and periodicity of cycles, including temporal autocorrelation, when the conditions at any time point are very similar to the conditions in the previous time) shapes biological responses and is fundamental for understanding and predicting the responses in the coastal ecosystems.

A range of coastal marine habitats including estuaries, salt marshes, kelp forests, and sea grasses experience considerable natural fluctuations in pH over diel timescales (e.g., 9, 25, 26). Because of higher pH_{max} conditions in these habitats, they are described as refugia for calcifying species against OA.[27] However, some studies also show a range of negative impacts

https://doi.org/10.1021/acs.est.2c00010
Environ. Sci. Technol. 2022, 56, 9015−9028

under pH variability, including lower shell defense capacity, susceptibility to predators and pathogens, and reduced fitness.[28−31] Shell biomineralization is recognized as one of the most sensitive processes to OA. Because of the subtle dynamics between shell dissolution and calcification, the balance between these processes is inextricably linked to the ecology of the calcifying species[32−37] because of the energetic costs.[38] Shell dissolution imposes negative impacts on the shell structure and function, organismal fitness, increased predation pressure, reduced production, and mechanical properties of byssal threads and energetic outcomes.[32,39−47] Bivalve shells are calcium carbonate ($CaCO_3$) composites embedded in the complex organic matrix (refs 37, 41, 48−50, and reference therein). The three-layered shell consists of the upper periostracum, which covers the outer prismatic and inner nacreous layers, where the crystals are structured in various spatial microstructures that characterize the shell structure, configuration, and function;[51] one of the most common is a "columnar calcite prismatic" layer, which occurs in the external shell of oysters. These calcite prisms are formed as individual polygons separated by an organic interprismatic membrane.[48,52,53] Despite concerns for economically important calcifiers under future variability in carbonate chemistry dynamics, mollusk shell dissolution remains a largely understudied process despite its adverse effects on essential processes like shell development and its function.[32,38]

With global production of 573,616 tonnes and an annual value of $19 billion USD globally,[54] oysters are one of the most important aquaculture species that are directly impacted by ocean acidification.[55−59] Oysters are a key foundation species,[60,61] providing habitat for a wide range of species and supporting key ecosystem services. The oyster industry in the US generates $186 million per annum.[62,63] The Pacific oyster, *Crassostrea gigas* (also called *Magallana gigas*), is one of the most "globalized" introduced species, largely due to its leading role in harvest production. In some cases, *C. gigas* has displaced native species and modified habitat processes.[64−66] In the western US, while the most important aquaculture species today is the Pacific oyster, aquaculture began with the native Olympia oyster (*Ostrea lurida*), a species that still remains an important contributor to regional oyster production and holds a strong cultural heritage appeal. Pacific and Olympia juvenile oysters live in intertidal habitats where they balance their fitness in context with diel pH variability and the predictability of environmental change. With the amplitude of the fluctuations predicted to increase in the near future[3,4] and environmental variation to become more fluctuating, that is, less unpredictable,[21] the extent to which the oysters will cope or adapt to coastal ocean changes is unknown.

The effects of changing means, amplitudes, and frequency on calcifying organisms can be simulated in laboratory settings, with the focus on investigating which mode of variability has the most impact on the biological responses. In this study, we examine how conditions related to variability impacted oyster biomineralogical and physiological (shell dissolution, calcification, growth, respiration, clearance rate, survival) responses. We exposed both species to experimental conditions that simulate both present-day and future conditions[4,5,9] over a period of 6 weeks. In an analysis of available data from the National Estuarine Research Reserve System (NERRS), we assessed the patterns of fluctuations, including the mean and the range of variation as well as predictability determined as a pattern of temporal pH autocorrelation across various northeast Pacific coast estuaries. Extrapolating the laboratory results to the field, we discuss how the unique signatures of pH variability impact oyster fitness within each of the estuaries.

2. METHODS

For all the analyses, we only provide a short description here, with an extended description of the analyses in the Supporting Information.

2.1. pH Data Analyses across the US Estuaries. Data were compiled from the seawater pH monitoring program of the US NERRS. Six estuaries along the US Pacific coast where the oyster are/were ecologically and/or economically important and for which sufficiently long pH time series from the NERRS exist. The following estuaries fulfilled all the criteria (from north to south): Kachemak Bay (AK), Padilla Bay (WA), South Slough (OR), San Francisco Bay (CA), Elkhorn Slough (CA), and Tijuana River (CA) (Figure 1; Table S1). Two stations were selected within each estuary, one at the outermost (seaward) and one at the innermost (landward) locations for May−September, representative of the growing period of the juvenile (spat stage) oysters in their natural habitat. The diel mean and range of pH were calculated from the continuous data.

2.2. Analysis of Diel pH Fluctuations and Predictability across the Pacific Coast Estuaries. Calculations of the integrated duration and intensity of diel pH variability (diel mean and diel ranges) were conducted using the approach described in Bednaršek et al.[10] Time series of pH were evaluated to characterize the dominant frequencies of variation and their amplitudes. The goals of the analysis were to (1) evaluate if the experimental treatments were reasonable approximations of real-world variability and (2) characterize predictability (temporal autocorrelation) patterns of environmental conditions for inference on the physiological response of biological organisms to pH variability; Figure S1). We used wavelet analysis to first identify dominant periods of cyclical periodicity in pH time series at the six NERRS sites for May−September 2019, following the transform package developed by Grinsted et al.[67] Wavelet analysis is a type of spectral analysis that shows how the variance spectrum of frequencies changes over time (e.g., a previous study[68]). It is particularly useful for the evaluation of the environmental predictability for sensitive marine organisms.[23] Using MATLAB R2021a using a continuous wavelet transform package, these results allowed us to identify the relative strengths of the frequency components, such as seasonal periodicity as compared to daily or subdaily periodicity (Figure S1). Once the dominant periods were identified from the wavelet analysis, the decomposition of the time series into separate (and additive components) for long-term (inter-annual or seasonal), daily, and subdaily (i.e., tidal) periodicity was done to quantify amplitudes attributed to each. (Figure S2). Ten years of data (2010 through 2019) were evaluated for each of the six NERRS sites. This was done stepwise by (1) predicting the annual/seasonal variation by modeling pH vs annual time using sine wave regression[69] and subtracting this from the observed time series, (2) predicting the daily amplitude using sine wave regression as an estimate of diel variation in pH related to biological productivity and subtracting this from the seasonally detrended time series, and (3) predicting the remaining variation attributed to tidal forcing with harmonic regression. The results provided an estimate of the amplitudes of isolated variance components acting at each time scale (Figure S3).

https://doi.org/10.1021/acs.est.2c00010
Environ. Sci. Technol. 2022, 56, 9015−9028

A)

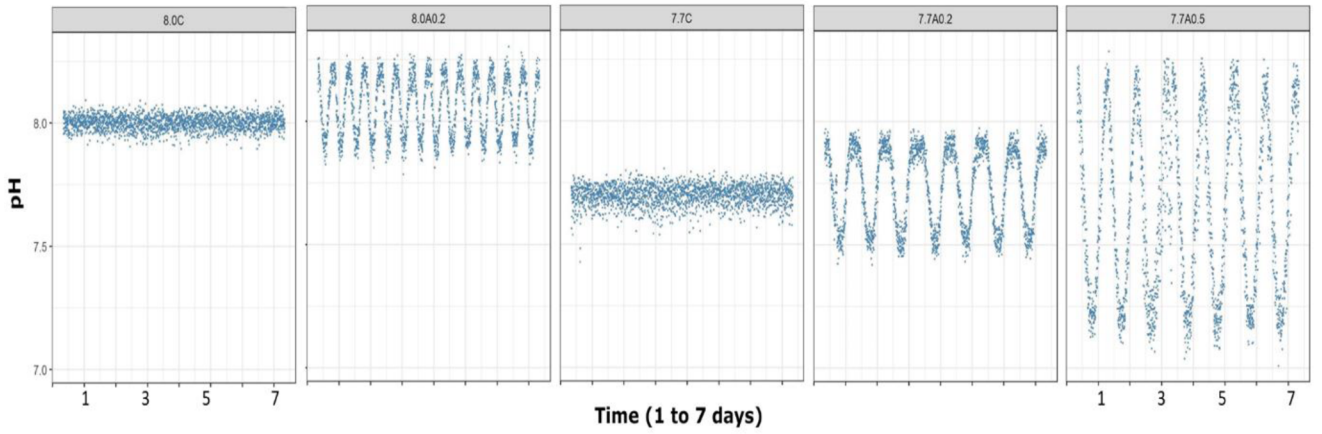

B)

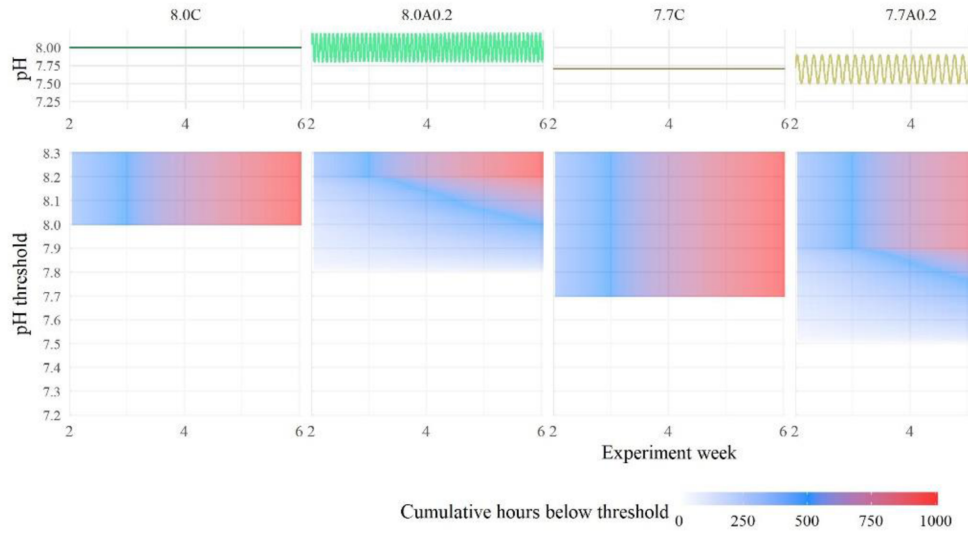

C)

Treatment Name	Type	Mean (pH)	Max (pH)	Min (pH)	Transition (h)	Hold (h)	Period (h)
pH7.7±0.5	Variable	7.7	8.2	7.2	7 h	5	24
pH7.7±0.2	Variable	7.7	7.9	7.5	7	5	24
pH8.0±0.2	Variable	8.0	8.2	7.9	5	1	24
pH=8.0	Static	8.0					
pH=7.7	Static	7.7					

Figure 2. Categorization scheme of different types of shell dissolution of the juvenile stages of both oyster species. The surface images of severity of dissolution under SEM show progression from the top to the bottom row. The first row depicts the outer intact prismatic region characterized by a smooth surface and some upper level of shell dissolution (Type I) presence; the second row shows the progression of dissolution to partially dissolved prismatic layer with mild to moderate dissolution (Type II); the third row is a depiction of the most severe shell dissolution (Type III) with a completely dissolved prismatic layer and partially exposed lower, cross-lamellar layer. The bars on each image indicate the magnification.

2.3. Manipulation of Seawater pH: Static and Fluctuating pH Treatments. Based on the in situ pH conditions, we designed six-week long experiments of a total of five pH_T (pH total) treatments. For future conditions, we used climate change projections for the year 2100 from Pacella et al.[4] (Tables S2 and S3; Figure S4). The experiments were as follows:

1. two "static" treatments (for current and future projected conditions; pH 8 and pH 7.7)
2. two "dynamic" treatments with a defined daily pH amplitude (pH 7.7 ± 0.2 and pH 7.7 ± 0.5)

https://doi.org/10.1021/acs.est.2c00010
Environ. Sci. Technol. 2022, 56, 9015−9028

3. one increased "frequency" treatment (pH 8.0 ± 0.2) with a shorter transition and hold time.

2.4. Experimental OA Exposures of Two Oyster Species. The experiments were conducted in the flow-through Dynamic Stressor Exposure Research Facility (DSERF) in which fluctuating conditions were set up and controlled through a series control solenoids and mass flow controllers using National Instruments (NI) hardware and Labview software to control for pH, dissolved oxygen, and temperature using a feedback mechanism of pH setpoint detection. The pH-adjusted seawater flowed by gravity to the exposure jars containing the oysters. For the dynamic aspect of the exposures, pH changes were programmed to occur in evenly distributed incremental adjustments to achieve the desired pattern of time at each pH for each treatment. We used juveniles of the Pacific oyster (*Crassostrea gigas*) and native Olympia oyster (*Ostrea lurida*). Oysters were fed twice daily with 400 μL of Shellfish Diet 1800 diluted 1:1 with seawater. We set up a total of 85 exposure jars (2 L) at the start of the experiment with each experimental treatment (5 treatments) in 5 replicates, that is, we controlled for the replication in the statistical analyses by using jars as a random effect. At weeks 2, 4, and 6, five jars from each treatment (25 jars per treatment) condition and the oysters contained within were used for biomineralogical and physiological assays. Water in the exposure jars was completely replenished every 2−4 h.

2.5. Oyster Shell Dissolution. The shells were cleaned for scanning electron microscopy (SEM) following previous studies,[51,70,71] using sodium hypochlorite (NaOCl, commercial bleach diluted to obtain 5% v/v NaOCl) for approximately 1−1.5 h. The growing edge of each shell was a newly grown surface area in each subsequent week, indicating new dissolution in weeks 2, 4, and 6. SEM was used to characterize shell dissolution. Shell dissolution was investigated in 190 Pacific oysters and 185 Olympia oysters from five different experimental treatments. Over the shell surface area, we randomly examined 10−25 regions with the examination started at one side of the growing edge, followed by a random choice of zooming out to a set magnification (600×) and panning through the field of view five times at 20−25 regions on the overall growing edge. Following the literature on the crystalline structure, we developed a categorization scheme (Figure 2) for oyster dissolution extent over the new growing area as follows:

Intact shell (*Type I dissolution*) indicates that the prism surfaces were mostly intact (*Type 0*) with a smooth appearance, or with surface dissolution in some organisms. In its intact form, the oyster exterior surface contains calcite crystals formed into polygons.[51] *Moderate dissolution* (*Type II dissolution*) involves a partially eroded outer prismatic layer with exposed crystals. When the crystals are exposed by the dissolution of the outer prismatic layer, they appear in the concentric, spherulitic shapes partially covered by the prismatic layer. *Severe dissolution* (*Type III dissolution*) builds off the Type II dissolution with a completely removed prismatic layer and partially exposed lower, cross-lamellar layer. The crystals are severely dissolved, characterized by the gaps in the crystalline structure. Approximately 10−20 SEM images were produced per individual on the external crystalline shell side, and each image was scored separately for the dissolution type (Type I to Type III). We used five individuals per jar to determine the extent of severity of dissolution, here referred to as the *Mean dissolution*, at the growing edge of each oyster (sensu 34).

2.6. Measurements of Shell Growth Analyses, Respiration, Clearance Rate, and Survival. We determined shell growth and calcification using both qualitative and quantitative methods; qualitatively, we used two different staining procedures at the growing edge using fluorescent dies calcein and calcofluor, with the region of new growing edge formed during the experimental exposure fluorescing after staining (Figure S6). We used 0.5 mg/L calcein and calcofluor for 16 h one day before the experiment ended in week 6 across all the treatments. Calcein was bound to the mineralizing shell and labeled the growing edge at the time of staining, while the calcofluor bound to the newly formed organic chitinous and proteinaceous layers to mark the area of the intense growing edge. Five oysters of each species per treatment were investigated with a Nikon Eclipse 90i microscope using UV blue excitation at 100× magnification. For quantitative estimates, we developed an artificial intelligence (AI) algorithm for image analyses and1735 Olympia and 1705 Pacific oysters. Image analysis methods were developed to facilitate the automatic measurement of the surface area of each individual in each image (see the Supporting Information). Respiration rates (oxygen consumption) were measured at weeks 2, 4, and 6 of the experiment in the respirometry chambers. The change in oxygen concentration inside the sealed chambers was measured using OXY-4 SMA multichannel oxygen meters fitted with fiber-optic probes.

Respiration was measured in eight individuals randomly collected from four exposure jars replicated in each of the five treatments (N = 40 individuals per species per sampling date). Incubations were run until a 10−15% decrease in oxygen concentration was observed. Oxygen consumption rates were calculated based on the change in oxygen concentration for each chamber, corrected for any background oxygen consumption, and normalized to wet tissue mass to account for any variation in size (oxygen consumed per hour per gram wet tissue mass (μmol h^{-1} g^{-1})).

Clearance rates were measured for both species of oysters in four of the experimental treatments and were defined as the volume of water cleared of particles per unit time, calculated indirectly from the measured decline in chlorophyll a (chl-a) concentration inside sealed incubation jars. Dead oysters were counted biweekly to construct survival curves using the *survival* package in and evaluated using the Kaplan−Meier estimate for right-censored data.

2.7. Statistical Analyses of the Experimental and Field Data. Changes in shell dissolution for each oyster species were analyzed by two-way analysis of variance (ANOVA) with treatment and duration as fixed factors, including an interaction between the two. The treatment jar was used as a random effect to account for residual variation attributed to factors other than treatment and week. All treatments were balanced, meaning that the same sample size was used to evaluate differences among treatments and weeks (fixed effects), with the same replicate jar effects modeled as random effects.

3. RESULTS

3.1. Diel pH Fluctuations across Coastal-Estuarine Habitats. Analyses of pH time series records from six coastal-estuarine habitats along the Pacific coast reveal that lower pH and diel variations are a common occurrence during May−

https://doi.org/10.1021/acs.est.2c00010
Environ. Sci. Technol. 2022, 56, 9015−9028

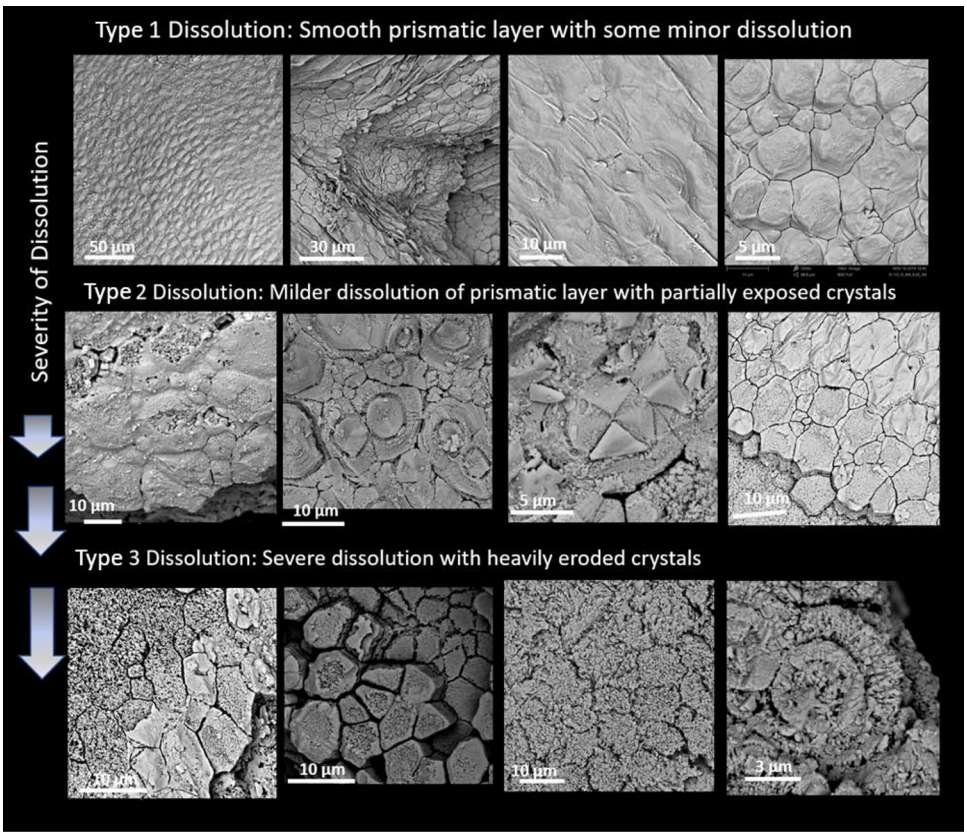

Figure 3. (A) Range of diel pH conditions across five different experimental treatments. Experiments included two static treatments (control pH = 8 and lower pH = 7.7); two dynamic treatments with a pH mean of 7.7 and a pH amplitude of 0.2 and 0.5 that define the minimum (Min) and maximum (Max) pH values (pH = 7.7 ± 0.5); and high-frequency treatment (pH = 8.0 ± 0.2) with shorter transition and hold time (Table S2). Depicted conditions are representative over one-week basis. Treatment indication on the top of the Figure. (B) Cumulative exposure across the experimental treatment. The top row shows the pH treatment, and the bottom row shows expected exposure time as cumulative hours below a given pH threshold shown on the *y*-axis for the duration of the experiment. (C) Targeted experimental conditions that span an average (Mean), different amplitudes for pH minimum (Min) and maximum (Max) values, the dynamic and frequency treatments characterized by the time to change to or from Min and Max (Transition) and time spent at the maximum or minimum pH (Hold), and the time for one full pH fluctuation cycle (Period).

September across all the estuaries; however, there are significant differences in the mean and amplitude of fluctuations among the estuaries, which is reflected in the exposure duration time and intensity below the thresholds (Table S1). Kachemak Bay, Padilla Bay, South Slough, and Elkhorn Slough experience pH lower than 7.7 very rarely, while pH values <7.7 represent common conditions in the habitats of the San Francisco Bay and Tijuana River, especially those on the inner estuarine side compared to those nearer the ocean (Figure 1, Table S1). Moreover, with exception of the Kachemak Bay, the estuaries regularly experience diel amplitudes of 0.2 and 0.5 around pH of 8, but not below. This is not the case for the conditions below pH 7.7 but is common for the San Francisco Bay and Tijuana River. The results of the decomposition analyses using 10-year data from estuarine conditions in the north−south direction reveal strong latitudinal differences in the variability, with estuaries to the north having higher mean pH values and smaller amplitude of variability. The extent of diel variability with increased amplitude and lower pH_{min} conditions increases southward, especially in the inner part of the estuaries (Figure 1, Table S1).

3.2. Temporal Predictability across the Estuarine Habitats. With the use of the wavelet, autocorrelation, and decomposition analyses (Figures S1−S3), we identified the relative strengths, frequency, and amplitude of variation that demonstrate the range of annual, seasonal, daily, and subdaily periodicity across all of the estuaries we studied. Results of the wavelet analyses (Figures S1 and S3) showed that diel frequencies were more predictable in more southerly locations, as anticipated, given an increase in temperature driving strong diurnal productivity patterns closer to the equator. Subdiel frequencies caused by tidal variation were also consistently observed at many of the NERRS sites, owing to the strongly mixed semidiurnal tidal components characteristic of the Pacific Coast. Some differences in the wavelet analyses between the inner and outer stations were also observed. For example, Padilla Bay's inner station (PDDBY) showed stronger diel frequencies than its outer station (PDBGS), likely related to the presence of eelgrass beds driving productivity patterns at the inner site. Decomposition analyses supported the results of the wavelet analyses by confirming the presence of increased amplitudes with strong latitudinal gradients in a southward direction, showing the transition from seasonal in the northern estuaries, to daily and subdaily in the southern estuaries (Figure S3). Along with the amplitude of variation, autocorrelation analyses show an increasing trend of predictability from the north to the south, as well as in the outer-inner direction of the specific estuary (Figure S2). In terms of predictability over the diel and subdaily scale, the

https://doi.org/10.1021/acs.est.2c00010
Environ. Sci. Technol. 2022, 56, 9015−9028

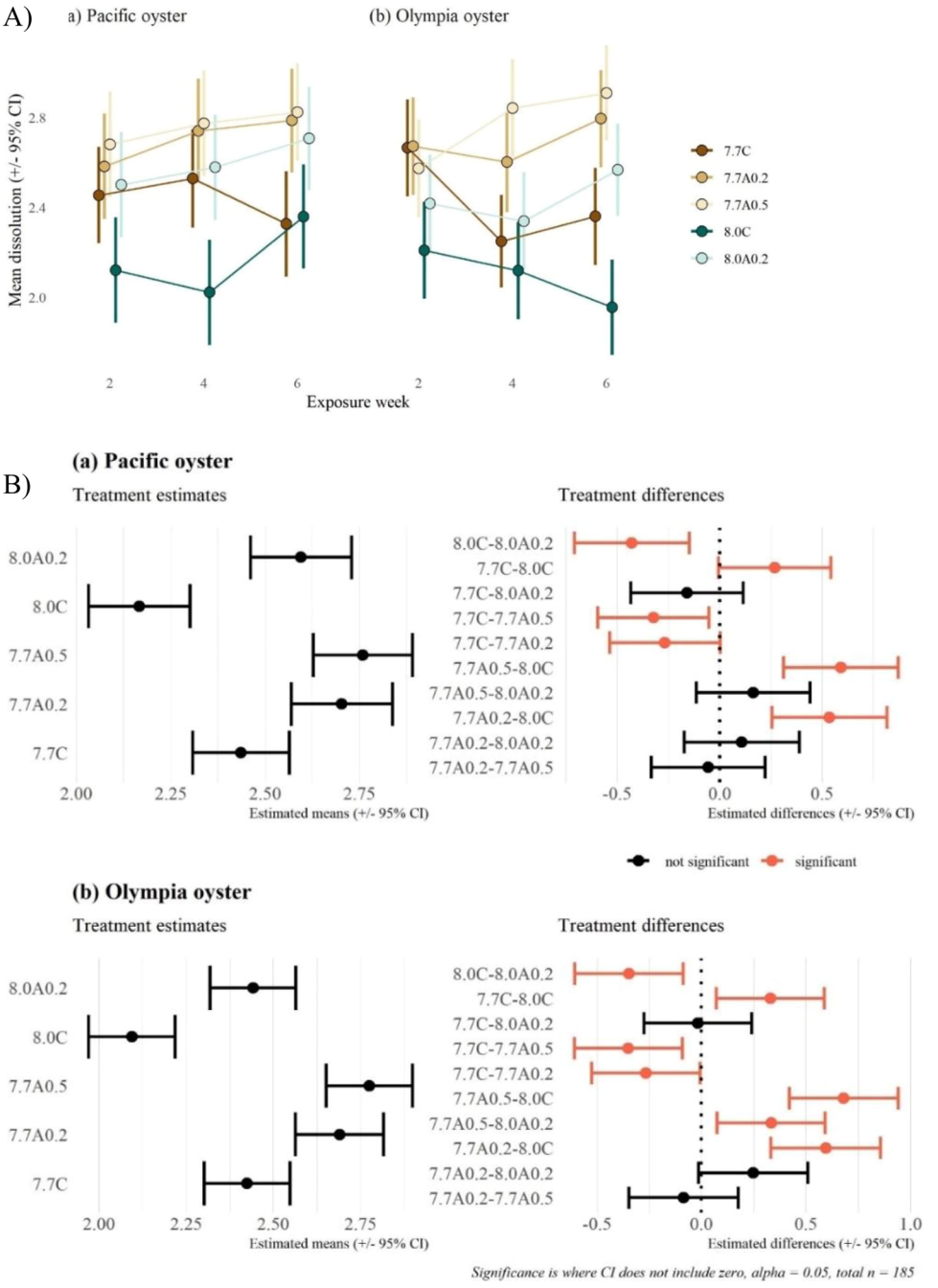

Figure 4. (A) Model estimates of mean dissolution (±95% confidence intervals) for each species (Pacific (a) and Olympia (b), treatment and week of experimental exposure (in weeks 2, 4, and 6). A total of 190 Pacific and 185 Olympia were used. Estimates are based on two-way analysis of variance models with an interaction between week and treatment, using jar as a random effect. Confidence intervals that do not include zero have statistically significant dissolution and treatments/weeks that have nonoverlapping confidence intervals can be considered statistically different. (B) Model estimates of mean dissolution by treatment across all weeks. Estimates are based on linear mixed effects models to test for differences in dissolution by treatment. The left plots show mean dissolution estimates from each model, and the right plots show post-hoc pairwise comparisons of mean differences between treatments. Confidence intervals in the right plot that do not include zero indicate pairs of treatments with significantly different dissolution means.

locations with the least productivity (least diel pH range; e.g., Kachemak Bay) tend to have the lowest predictability of the long term, with nearly zero autocorrelation after 2 weeks. We note that Kachemak Bay, with very low diel variation in pH, is still highly predictable over shorter time scales (up to several days), but less predictable than other locations over longer time scales (several weeks) compared with other locations. In contrast, the locations with the greatest productivity (inner Padilla Bay, South Slough, Elkhorn, and Tijuana River) have the greatest diel predictability with temporal autocorrelation coefficients of around 0.5 after 2 weeks (Figure S2), where diel periodicity can be easily quantified and is therefore predictable biologically.

3.3. Dynamic OA Conditions in the Experimental Treatment. The mean, diel minimum and maximum extremes, and the range of variability in pCO_2, pH_T, carbonate

https://doi.org/10.1021/acs.est.2c00010
Environ. Sci. Technol. 2022, 56, 9015−9028

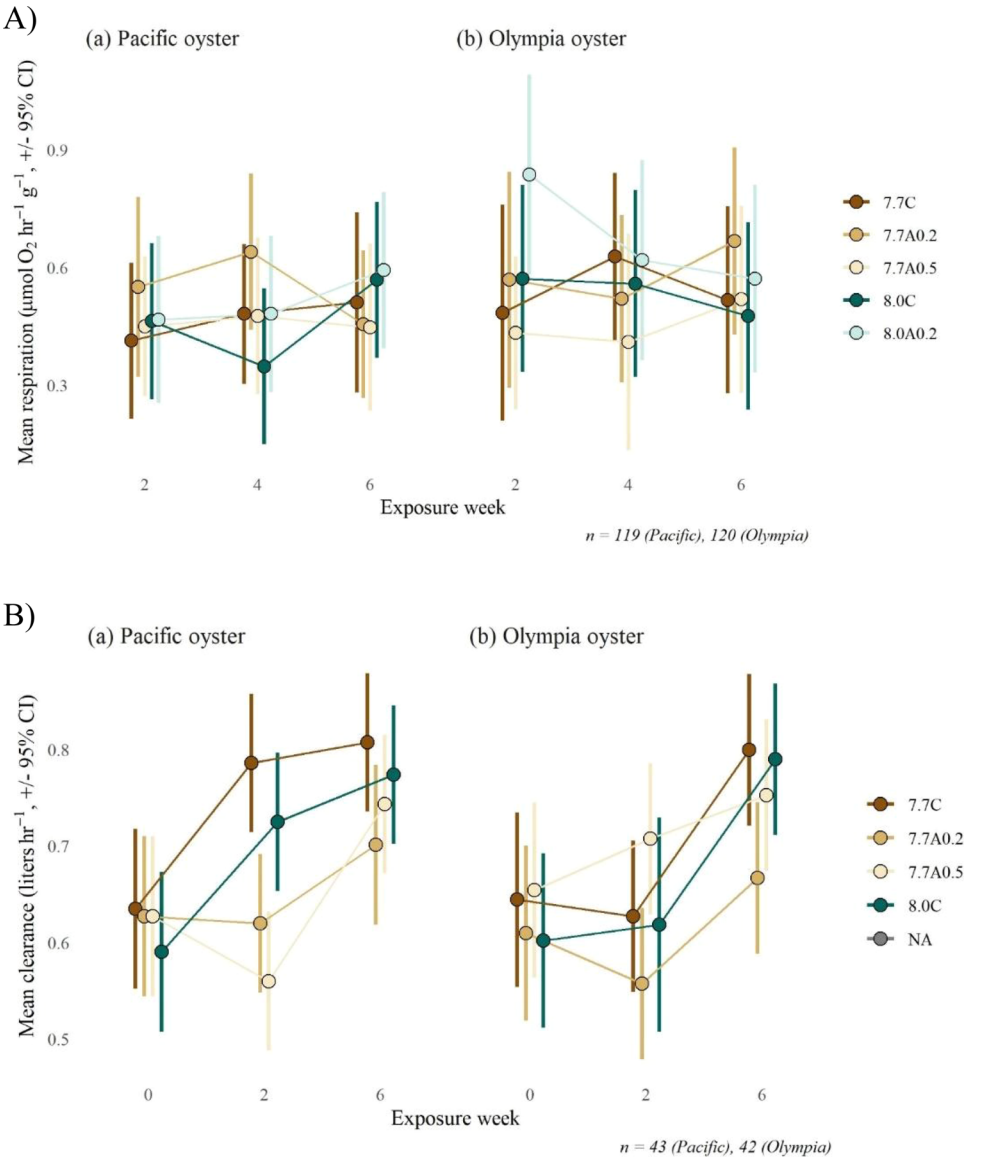

Figure 5. (A) Respiration rates (upper panel; measured as oxygen consumption: μmol O_2 h^{-1}) and (B) clearance rates (lower panel; L h^{-1}) with ±95% confidence intervals for each species (Olympia and Pacific oyster), treatment, and week of experimental exposure. Number of assays for respiration: N = 6−10 assays of individual oysters; for clearance: N = 2−4 independent assays per treatment. Estimates are based on the two-way analysis of variance model with fixed effects for week and treatment. Confidence intervals that do not include zero have statistically significant clearance and treatments/weeks that have nonoverlapping confidence intervals can be considered statistically different.

ion concentration, and aragonite/calcite saturation state (Ω_{ar}, Ω_{cal}) of the experimental conditions, along with auxiliary environmental data, are presented in Table S3 and Figure 3. The conditions of calcite near- or undersaturation ($\Omega_{cal} \leq 1$; pH = 7.55) were reached in one fluctuating experiments characterized by the greatest amplitude (pH 7.7 ± 0.5). The experimental treatments differed in the duration of cumulative exposure below a specific pH threshold (Figure 3B), with greater amplitude in the fluctuating treatments, resulting in prolonged cumulative exposure time compared to the static treatments at the same pH. The duration of exposure to less-favorable conditions increased in the following order: pH 8 > pH 8.0 ± 0.2 > pH 7.7 > pH 7.7 ± 0.2 > pH 7.7 ± 0.5 (Figures 3 and S4).

Various experimental conditions represented the range of current mean and extreme conditions found in the Pacific coast estuaries (Tables S1 and S2). The treatments of pH 7.7 with the amplitudes ±0.2 and ± 0.5 are representative of future projected conditions (sensu 4). All of the treatments resembled the temporal variation of conditions experienced in situ, except for the high-frequency treatment, where the periodicity of the exposure over the 96 h period (Figure 3) with lower autocorrelation, making this an "unpredictable" treatment (Figures S4 and S5).

3.4. Comparison of Shell Dissolution under Various Treatments. Under control, that is, static conditions (pH 8), SEM imaging of the external prismatic layer revealed that the intact calcite crystals are well-structured and arranged in polygons, with the outer crystalline surface being mostly intact. We note that in some individuals or parts of the growing edges, higher extent of Type I in combination with Type II dissolution was evident, pointing to a greater variability among the individuals and spatial dissolution on the growing edge. Taking the variability in the control (pH 8) into account,

https://doi.org/10.1021/acs.est.2c00010
Environ. Sci. Technol. 2022, 56, 9015−9028

the mean dissolution of around 2 (± 95% CI) can be considered as a baseline status under no stress, with subsequent increases up to mean dissolution of 2.75 (95% CI), representing the stress response under more stressful conditions (Figure 4). Compared to the control treatment, the mean dissolution in both species showed significant responses related to the treatment, but there were no differences in response by week; all treatments were considered equal over the timeframe of the experiments. There were also no significant differences between the species ($p > 0.05$ for all comparisons) (Figure 4, Table S4).

There are several high-amplitude and high-frequency dissolution-related patterns that were observed. First, mean shell dissolution significantly increased under the lower pH static (pH 7.7) treatment compared to the control (pH 8). Second, the diel fluctuations increased dissolution compared to the static treatments (pH 7.7 vs 7.7 ± 0.2; pH 7.7 vs 7.7 ± 0.5; pH 8.0 vs 8.0 ± 0.2; $p < 0.05$ as shown in treatment differences, Figure 4). Third, low pH with amplitude induced the most dissolution compared to the other treatments (e.g., 7.7 ± 0.2 and 7.7 ± 0.5 vs pH 8.0 and pH 7.7). Fourth, the amplitude of variability did not significantly impact dissolution. Fifth, even calcite-supersaturated conditions (Ω_{cal} of 2 corresponding to pH = 7.75) induced significant dissolution. Sixth, high-frequency (pH 8.0 ± 0.2) exposure results in significantly higher dissolution compared to the control (pH 8, $p < 0.05$), but a similar amount of dissolution to pH 7.7 or pH 7.7 ± 0.2 ($p > 0.05$, Figure 4).

Severity of dissolution is related to the mean and the amplitude of exposure, increasing with lower pH, higher amplitude of variability, as well as the combination of both parameters, i.e., low pH with high amplitude, associated with prolonged cumulative exposure (Figures 3 and S4). This explains significantly larger dissolution in pH 7.7 compared to pH 8, pH 7.7 ± 0.2 and pH 7.7 ± 0.5 compared to pH 7.7, and pH 8.0 ± 0.2 compared to pH 8 (Figure 4). However, it does not explain comparable dissolution in pH 8.0 ± 0.2 to pH 7.7 or pH 7.7 ± 0.2 despite prolonged cumulative exposure at lower pH for the latter two. This indicates that greater mean shell dissolution in the high-frequency treatment is not related to the variability but to the low autocorrelations of the conditions. Despite a substantially longer cumulative exposure time in the pH 7.7 ± 0.5 treatment, both oyster species did not show significantly increased shell dissolution compared to that of the pH 7.7 ± 0.2 treatment over six-week exposure. This result indicates a potential threshold at pH 7.7 ± 0.2 ($\Omega_{cal} \sim 2$), with significantly greater dissolution occurring in both species. Field conditions across the estuaries indicate that increased shell dissolution related to a higher amplitude of variability would be expected in the estuaries along the California coast and across the inner sides of all the estuaries except for Alaska (Figures 1 and S3, Table S1), particularly at longer (i.e., seasonal) exposure duration.

3.5. Calcification and Growth Process under Various Experimental Treatments. Fluorescent images of the oyster's growing edges using calcein show calcium carbonate deposition; calcofluor was attached on the chitin of the growing edge, demonstrated as blue fluorescence of the growing edge; the stains combined indicated the accretion of the inorganic (carbonate) and organic component at the growing edge across various experimental treatments (Figure S6). Continuous calcification was maintained throughout the entire duration exposure in all experimental treatments (Figures S6 and S7). The estimates of the mean calcification (in % ± 95% CI) show no treatment- or duration-related differences for both species ($p > 0.05$; Figure S7, Table S5).

The quantification of the oyster inorganic and organic growth, which was done by separately measuring the length and weight, demonstrated only a few significant differences in the size (shell surface area) or mass (whole animal mass) for either species of oysters ($N = 1735$ Olympia, $N = 1705$ Pacific) over the observed period of exposure (Figure S8). For nearly all treatments, Olympia spats were significantly larger than those of the Pacific oyster (shell surface area: $F = 1077$, $p < 0.001$; shell mass: $F = 1153$, $p < 0.001$; tissue mass: $F = 256.3$, $p < 0.001$) at the end of the experiments. There were no significant effects of the treatment group on tissue mass for the Olympia ($F = 0.79$, $p = 0.54$) or the Pacific ($F = 0.68$, $p = 0.61$) oyster. Also, no significant differences in size were detected by treatment for the Olympia ($F = 0.86$, $p = 0.49$) or Pacific ($F = 0.32$, $p = 0.86$) oysters across each week (Figure S8).

3.6. Respiration. Respiration rates of oyster spat were measured as oxygen consumption (Table S6, Figure 5). Incubation times ranged from 6 to 12 h, and the decline in oxygen concentration was highly linear during incubations for both Olympia ($R^2 = 0.96$; $p = 0.006$; $N = 121$ independent respirometry assays) and Pacific ($R^2 = 0.97$; $p = 0.004$; $N = 121$ independent respirometry assays) oysters. During the experiment, respiration did not differ significantly in response to the experimental treatment or the duration of exposure (week during experiment) for either species. However, respiration rates were significantly different between species overall, with oxygen consumption higher for Olympia oysters relative to Pacific oysters.

3.7. Clearance Rates. Clearance rates increased significantly by the end of the six-week experiment and differed between some treatments (Figure 5, Table S7). ANOVA shows a significant main effect of week (elapsed time during experiment) and treatment, with no interaction between the two. Subsequent comparisons indicate that clearance rates were significantly greater during week 6 of the experiment relative to the initial ($p < 0.001$) or week 2 ($p < 0.001$) measurements. The final analysis combining week × treatment × species shows that there is no difference in clearance rates between species.

3.8. Survival. Mortality of both species ranged between 6 and 8% across the weeks and treatments, with total mortality by week 6 being 10% (Pacific, pH 8.0) to 20% (Olympia, pH 7.7) of the values at the beginning of the experiment. Within a species, Kaplan–Meier survival estimates (Figure S9) showed no statistical differences across treatments ($\chi 2 = 2.1$; df = 4; $p = 0.7$ for Olympia; $\chi 2 = 2.3$; df = 4; $p = 0.7$ for Pacific), nor between species within treatments ($\chi 2 = 1.1$; df = 1; $p = 0.3$).

4. DISCUSSION

Predictions of significantly greater variability in coastal waters due to nonlinear carbonate chemistry, in particular the buffering capacity,[3,4] prompted the investigation of the biological ramifications for two ecologically and economically essential oyster species (*Crassostrea gigas*, *Ostrea lurida*). While our understanding of the physical–chemical component of OA in the highly variable coastal intertidal habitats is progressing, the biological OA field is still hindered by poor understanding of the impacts due to variability, highlighting the importance of predictability of environmental changes and periodicity of cycles. This is despite extensive theoretical and empirical work

https://doi.org/10.1021/acs.est.2c00010
Environ. Sci. Technol. 2022, 56, 9015−9028

in other systems, indicating that the amplitude of fluctuations may be less important to that of the predictability in determining how organisms respond to environmental variations.[21,22,24] This study focused on experimental conditions corresponding to the variability and variation found in the Pacific coast estuaries.

Our results show increased shell dissolution under low pH and higher amplitudes of variability, as well as under less-predictable (low autocorrelation) conditions. Considering the drivers behind dissolution, the magnitude and duration of exposure were taken into account. For example, while dissolution was expected to be most prevalent in the undersaturated conditions that were present only in the pH 7.7 ± 0.5 treatment (Ω_{cal} < 1.8; pH < 7.4), dissolution was also prevalent in the supersaturated conditions found in the experimental treatments of pH 7.7, pH 7.7 ± 0.2, and pH 8.0 ± 0.2 (Table S3). With respect to the duration of exposure, increased occurrence of shell dissolution in the fluctuating versus static treatments (Figure 4) points to the importance of amplitude-related fluctuations with a prolonged duration as a driver behind biological responses. Both fluctuating experiments, that is, pH 7.7 ± 0.2 and 7.7 ± 0.5, triggered similar severity of dissolution despite the exposure to lower pH values although at a shorter cumulative duration in pH 7.7 ± 0.5. It is possible that the overall six-week experimental exposure was not sufficient to delineate the differences between the two treatments. Duration exposure, even at the shorter duration in 7.7 ± 0.2, initiates the dissolution process, including the loss of periostracum[72−74] and Type I, II dissolution of the upper prismatic layer. Accounting for the dissolution kinetic algorithms,[75] prolonged exposure to $\Omega_{cal} \leq 1$ values in the fluctuating treatments accelerated the dissolution rates exponentially and resulted in significantly greater damage than that was expected from the linear process found under static conditions at $\Omega_{cal} > 1$. In addition, with the level of calcification remaining the same across the treatments (Figure S7), a prevailing process of shell dissolution over calcification is suggested. Surprisingly, a high-frequency treatment (pH 8.0 ± 0.2) triggered significantly more dissolution than that was expected based on the pH/Ω_{cal} magnitude or the exposure duration (Table S2; Figure S4). While the conditions in this treatment were not unfavorable for oysters, this treatment was characterized by altered frequency (low autocorrelation), in which the organisms could not rely on a priori predictable frequencies of variation. Despite these conditions, the organisms maintained their same level of calcification (Figure S7); thus, it is possible that other types of change in the shell occur. These could include chemical, elemental composition, and microskeletal property alterations,[76,77] or a change in protein expression and carbonic anhydrase activity,[41] with such multifaceted changes possibly leading to functional impairments and negative implications for shell material properties.[70,78] In time, the more porous, deformed, and fragile shells may inhibit the oysters' ability to withstand physical disturbances (e.g., 46), leading to increased predation.[79] Ecological implications over time could include the reduced height of oyster reefs and reef topography, an important consideration in the context of biogenic reef formations that attract and sustain biodiversity.[80] A focus on less-predictable future conditions, integrating molecular-level changes with microstructural and mechanical analyses is recommended as a next step in research.

There is consistent agreement across current studies that shell dissolution will be one of the most predominant problems for a wide group of calcifiers; here, we consider this specifically in the context of various oyster species, even when all the other physiological responses were not impaired.[47,71,72,81] Against the background of projected changes,[3,4] building and maintaining carbonate structures will thus depend on the balance between shell calcification and dissolution. Given that calcification is under strong biological control, oysters could maintain their calcification process because they are able to compensate against predictable pH fluctuations, but this may not be the case in less-predictable habitats, which would likely tip this balance in favor of dissolution. On the other hand, shell dissolution could exceed calcification because it is a faster process and likely bears higher energetic costs required for compensation,[38] as evident in carbohydrate and lipid metabolism changes.[82] Across the treatments, our results of increased clearance rate over time in both species would suggest increased intake of metabolic substrates to support greater energy production. We did not, however, detect a corresponding change in whole animal metabolic energy (respiration). In our experiments, despite a daily feeding regime with a recommended nutritional value, we allow the possibility that the construction of the meshed bags in which the oysters were kept did not always allow the organisms to be fed ad libitum, or at least not the ones that were deep in the meshed bags. While this more closely reflects the natural environment where food is not always in excess, it might also indicate the onset of energetic constraints. Recorded physiological tolerance (no change in response) related to calcification and metabolism (growth, respiration, and clearance) and survival in both oyster species differ from the results of earlier studies (e.g., ref 82). Such physiological resilience is determined by the species-specific critical thresholds related to physiological impairments, which were obviously not triggered in this study. From the variability perspective, such tolerance was not expected because these oysters did not experience similar fluctuations in nature. While the larval batch originated from the hatcheries, these oysters were subsequently outplanted into the natural conditions of Puget Sound (Pacific Northwest; mimicking the conditions in Padilla Bay), where the fluctuations are centered around pH 8 but not below 7.7.

The results of wavelet and decomposition analyses demonstrate that the Pacific coast estuaries are important natural analogues with variability patterns, including predictability. There is a strong latitudinal pattern of diel and subdiel variability and autocorrelation, both increasing latitudinally southward (Figures S2 and S3). Thus, while southern estuaries experience greater variability, they are also characterized by highly predictable diel frequencies of variation, indicating the complexity of biologically significant parameters in these habitats. This also means that the oysters from highly predictable habitats, contrary to the ones from northern habitats, may be more adaptable to predicted change and therefore better suited to sustain future changes related to variability. When considering the impacts of future conditions on biological responses, our results show that the fluctuating habitats with increasing amplitudes of variability will pre-expose the organisms to lower pH values more frequently and for prolonged cumulative durations.[3,4] In addition to considering mean pH and variance, it is crucial to evaluate the spatial−temporal variability for any given pH values and

https://doi.org/10.1021/acs.est.2c00010
Environ. Sci. Technol. 2022, 56, 9015−9028

include this interpretation while evaluating the impacts at different NERRS sites. This raises an important distinction related to various habitats in terms of predicting biological responses: first, habitats with similar means but different variance components need to be interpreted differently when considering exposure impacts; second, biological responses in habitats with high autocorrelation will likely be notably different from those in habitats with low autocorrelation (low predictability). For better prediction of biological responses, parameters such as amplitude of fluctuations, frequency, lowest pH/Ω conditions, the frequency of exposure, as well as cumulative exposure, and the determination of dominant frequencies of variation and amplitude of exposure in combination with the temporal variation of other stressors (sensu[83]) should be reported. It is of critical importance to disentangle the influence of each of these factors on species' responses and integrate them in the multiple stressor context.

Future studies should focus on these natural analogues to predict population outcomes more accurately, because the observed results align well with theoretical expectations that plasticity is favored in environments that fluctuate predictably.[19,20,22,23] Such comparative field studies would provide insights into the mechanisms underlying adaptation/plasticity while also keeping in mind that multistressor factors such as increasing temperature, increasing stratification, or decreasing oxygen may interact with pH variability (sensu[34,84]). Our results have important implications for decision-making processes concerning the oyster aquaculture industry and oyster reef restoration by pointing to the locations of potentially more resilient oyster populations and the locations that are most conducive (i.e., lower amplitude in variability and higher predictability) to oyster aquaculture. Interestingly, while considering the responses between introduced and native species, we did not find differences between the two species, indicating that it is not OA per se but likely a combination of interactive multiple stressors that trigger different sensitivities[85] and carry-over OA effects across life stages.[57]

Finally, potential mitigation and carbon dioxide removal (CDR) strategies for OA, like macrophytes and ocean alkalinity enhancement (OAE), can substantially modulate carbonate conditions. For macrophytes, reported studies[9,25,86−89] include an increase in mean or pH amplitude,[26,86,90−92] to which Wahl et al.[93] showed increased calcification processes in the macrophyte habitat. pH fluctuating habitats have recently gained recognition as potential OA refugia (e.g., ref 27), but the results of this study do not suggest any such benefits, recognizing that pH increase might not be sufficient to reduce shell dissolution. Instead, other factors related to variability, with an amplitude of variability and positive autocorrelation patterns, need to be strongly considered when designating habitats' role as OA refugia, with comprehensive biological assessments to guide such decisions. For future CDR mitigation strategies, OAE could be a suitable treatment. Given the fact that highly variable habitats have low buffering capacity,[3,4] increased total alkalinity increases the buffering capacity while decreasing the amplitude of variability. For many calcifiers for which dissolution has been recognized as a predominant problem under future scenarios of coastal acidification, OAE might reduce the severity of dissolution and increase the overall fitness of these mollusks and the ecosystems to which they contribute.

■ ASSOCIATED CONTENT

Supporting Information

The Supporting Information is available free of charge at https://pubs.acs.org/doi/10.1021/acs.est.2c00010.

Wavelet magnitude scalogram with frequency in terms of period; temporal autocorrelation analyses of the conditions during May−September 2019; results from decomposed pH time series from 2010 to 2020 at six NERRS sites; summary statistics of pH at six NERRS sites; conditions in the experiments with respective amplitudes; cumulative exposure (days, y-axis) across the duration of all conducted experimental treatments; temporal autocorrelation analyses of the experimental data; calcofluor and calcein staining of the growing edge in both oysters; model estimates of mean calcification; measurements of the final size (cm^2), shell weight (g), and tissue weight (g); survival estimates of oysters by species and treatment; analysis of variance for both oyster dissolution as a week by treatment interactions; analysis of variance mean calcification estimates for both oyster species as a week by treatment interaction; and analysis of variance details. (PDF)

■ AUTHOR INFORMATION

Corresponding Author

Nina Bednaršek − *Southern California Coastal Water Research Project, Costa Mesa, California 92626, United States; National Institute of Biology, Marine Biological Station, 6330 Piran, Slovenia;* Present Address: Cooperative Institute for Marine Ecosystem and Resources Studies, Oregon State University, Newport OR 97365, USA; orcid.org/0000-0002-9177-6626; Email: nina.bednarsek@nib.si

Authors

Marcus W. Beck − *Tampa Bay Estuary Program, St. Petersburg, Florida 33701, United States;* orcid.org/0000-0002-4996-0059

Greg Pelletier − *Southern California Coastal Water Research Project, Costa Mesa, California 92626, United States*

Scott Lee Applebaum − *Environmental Studies Program, University of Southern California, Los Angeles, California 90089, United States*

Richard A. Feely − *NOAA Pacific Marine Environmental Laboratory, Seattle, Washington 98115, United States*

Robert Butler − *Southern California Coastal Water Research Project, Costa Mesa, California 92626, United States*

Maria Byrne − *School of Life and Environmental Sciences, University of Sydney, Sydney 2006 New South Wales, Australia*

Betsy Peabody − *Puget Sound Restoration Fund, Bainbridge Island, Washington 98110, United States*

Jonathan Davis − *Pacific Hybreed, Inc., Port Orchard, Washington 98366, United States*

Jasna Strus − *Biotechnical Faculty, University of Ljubljana, 1000 Ljubljana, Slovenia*

Complete contact information is available at: https://pubs.acs.org/10.1021/acs.est.2c00010

Author Contributions

N.B. has written the manuscript. M.W.B. conducted statistical analyses with the involvement of N.B. S.L.A. provided

https://doi.org/10.1021/acs.est.2c00010
Environ. Sci. Technol. 2022, 56, 9015−9028

guidance in respiration measurements and analyses. R.A.F provided guidance on the carbonate chemistry measurements and analyses. G.P. conducted the analyses on the estuarine data. R.B. conducted AI work analyses. J.D. provided oysters. All the other authors have contributed to the writing or editing.

Notes

The authors declare no competing financial interest.

The datasets supporting this article will be uploaded as part of the NOAA/NCEIs database upon publication of this manuscript.

■ ACKNOWLEDGMENTS

This work was funded by Paul G. Allen Family Foundation. We thank Paul Smith for streamlining AI work protocols, Jude Apple provided guidance on access to data from NERRS, SCCWRP part-timers, Miloš Vittori (Biotechnical Faculty, Slovenia) conducted staining in the laboratory; Miranda Roethler and Merna Ewad are thanked for helping in laboratory work and laboratory analyses, Steve Bay and Darrin Greenstein for facilitating building experimental treatment and for maintaining experimental conditions and additional laboratory analyses. Nina Bednaršek acknowledges support from the Slovene Research Agency (ARRS "*Biomarkers of subcellular stress in the Northern Adriatic under global environmental change*", project # J12468). Nina Bednaršek and Jasna Štrus would like to acknowledge the financial support from the Slovenian Research Agency (bilateral project Slovenia-United States of America: BI-US/18-20-081). This is Publication Number 5165 from the Pacific Marine Environmental Laboratory of NOAA. We are grateful to the reviewers for their inspiring and useful comments that helped us make this manuscript much broader in its interpretation.

■ REFERENCES

(1) García-Reyes, M.; Largier, J. Observations of increased wind-driven coastal upwelling off central California. *J. Geophys. Res. Oceans* **2010**, *115*, No. 005576.

(2) Shaw, E. C.; Munday, P. L.; McNeil, B. I. The role of CO_2 variability and exposure time for biological impacts of ocean acidification. *Geophys. Res. Lett.* **2013**, *40*, 4685−4688.

(3) Feely, R. A.; Okazaki, R. R.; Cai, W. J.; Bednaršek, N.; Alin, S. R.; Byrne, R. H.; Fassbender, A. The combined effects of acidification and hypoxia on pH and aragonite saturation in the coastal waters of the California current ecosystem and the northern Gulf of Mexico. *Cont. Shelf Res.* **2018**, *152*, 50−60.

(4) Pacella, S. R.; Brown, C. A.; Waldbusser, G. G.; Labiosa, R. G.; Hales, B. Seagrass habitat metabolism increases short-term extremes and long-term offset of CO_2 under future ocean acidification. *Proc. Natl. Acad. Sci. U. S. A.* **2018**, *115*, 3870−3875.

(5) Cai, W.-J.; Feely, R. A.; Testa, J. M.; Li, M.; Evans, W.; Alin, S. R.; Xu, Y.-Y.; Pelletier, G.; Ahmed, A.; Greeley, D. J.; Newton, J. A.; Bednaršek, N. Natural and anthropogenic drivers of acidification in large estuaries. *Annu. Rev. Mar. Sci.* **2021**, *13*, 23−55.

(6) Cooley, S. R.; Doney, S. C. Anticipating ocean acidification's economic consequences for commercial fisheries. *Environ. Res. Lett.* **2009**, *4*, No. 024007.

(7) Cooley, S. R.; Lucey, N.; Kite-Powell, H.; Doney, S. C. Nutrition and income from molluscs today imply vulnerability to ocean acidification tomorrow. *Fish* **2012**, *13*, 182−215.

(8) Gattuso, J.-P.; Magnan, A.; Billé, R.; Cheung, W. W. L.; Howes, E. L.; Joos, F.; Allemand, D.; Bopp, L.; Cooley, S. R.; Eakin, C. M.; Hoegh-Guldberg, O.; Kelly, R. P.; Pörtner, H.-O.; Rogers, A. D.; Baxter, J. M.; Laffoley, D.; Osborn, D.; Rankovic, A.; Rochette, J.; Sumaila, U. R.; Treyer, S.; Turley, C. Contrasting futures for ocean and society from different anthropogenic CO_2 emissions scenarios. *Science* **2015**, *349*, No. aac4722.

(9) Baumann, H.; Wallace, R. B.; Tagliaferri, T.; Gobler, C. J. Large natural pH, CO_2 and O_2 fluctuations in a temperate tidal salt marsh on diel, seasonal, and interannual time scales. *Estuaries Coasts* **2015**, *38*, 220−231.

(10) Bednaršek, N.; Newton, J. A.; Beck, M. W.; Alin, S. R.; Feely, R. A.; Christman, N. R.; Klinger, T. Severe biological effects under present-day estuarine acidification in the highly variable estuarine regime of the Salish Sea. *Sci. Total Environ.* **2021**, *765*, No. 142689.

(11) Feely, R. A.; Alin, S. R.; Newton, J.; Sabine, C. L.; Warner, M.; Devol, A.; Krembs, C.; Maloy, C. The combined effects of ocean acidification, mixing, and respiration on pH and carbonate saturation in an urbanized estuary. *Estuar. Coast. Shelf Sci.* **2010**, *88*, 442−449.

(12) Evans, W.; Pocock, K.; Hare, A.; Weekes, C.; Hales, B.; Jackson, J.; Gurney-Smith, H.; Mathis, J. T.; Alin, S. R.; Feely, R. A. Marine CO_2 patterns in the northern Salish Sea. *Front. Mar. Sci.* **2019**, *5*, 536.

(13) Caldeira, K.; Wickett, M. E. Anthropogenic carbon and ocean pH. *Nature* **2003**, *425*, 365.

(14) Duarte, C. M.; Hendriks, I. E.; Moore, T. S.; Olsen, Y. S.; Steckbauer, A.; Ramajo, L.; Carstensen, J.; Trotter, J. A.; McCulloch, M. Is ocean acidification an open-ocean syndrome? Understanding anthropogenic impacts on seawater pH. *Estuaries Coasts* **2013**, *36*, 221−236.

(15) Cai, W.-J.; Huang, W.-J.; Luther GW 3rd; Pierrot, D.; Li, M.; Testa, J.; Xue, M.; Joesoef, A.; Mann, R.; Brodeur, J.; Xu, Y.-Y.; Chen, B.; Hussain, N.; Waldbusser, G. G.; Cornwell, J.; Kemp, W. M. Redox reactions and weak buffering capacity lead to acidification in the Chesapeake Bay. *Nat. Commun.* **2017**, *8*, 369.

(16) Fassbender, A. J.; Sabine, C. L.; Palevsky, H. I. Nonuniform ocean acidification and attenuation of the ocean carbon sink. *Geophys. Res. Lett.* **2017**, *44*, 8404−8413.

(17) Kwiatkowski, L.; Orr, J. C. Diverging seasonal extremes for ocean acidification during the twenty-first century. *Nat. Clim. Change* **2018**, *8*, 141−145.

(18) Lowe, A. T.; Bos, J.; Ruesink, J. Ecosystem metabolism drives pH variability and modulates long-term ocean acidification in the Northeast Pacific coastal ocean. *Sci. Rep.* **2019**, *9*, 963.

(19) Moran, N. A. The evolutionary maintenance of alternative phenotypes. *Am. Nat.* **1992**, *139*, 971−989.

(20) Reed, T. E.; Waples, R. S.; Schindler, D. E.; Hard, J. J.; Kinnison, M. T. Phenotypic plasticity and population viability: the importance of environmental predictability. *Proc. Roy. Soc. B* **2010**, *277*, 3391−3400.

(21) Botero, C. A.; Weissing, F. J.; Wright, J.; Rubenstein, D. R. Evolutionary tipping points in the capacity to adapt to environmental change. *Proc. Natl. Acad. Sci.* **2015**, *112*, 184−189.

(22) Bitter, M. C.; Kapsenberg, L.; Silliman, K.; Gattuso, J. P.; Pfister, C. A. Magnitude and predictability of pH fluctuations shape plastic responses to ocean acidification. *Am. Nat.* **2021**, *197*, 486−501.

(23) Bernhardt, J. R.; O'Connor, M. I.; Sunday, J. M.; Gonzalez, A. Life in fluctuating environments. *Philos. Trans. Roy. Soc. B* **2020**, *375*, No. 20190454.

(24) Bitter, M. C.; Wong, J. M.; Dam, H. G.; Donelan, S. C.; Kenkel, C. D.; Komoroske, L. M.; Nickols, K. J.; Rivest, E. B.; Salinas, S.; Burgess, S. C.; Lotterhos, K. E. Fluctuating selection and global change: A synthesis and review on disentangling the roles of climate amplitude, predictability and novelty. *Proc. Roy. Soc. B* **2021**, *288*, No. 20210727.

(25) Hofmann, G. E.; Smith, J. E.; Johnson, K. S.; Send, U.; Levin, L. A.; Micheli, F.; Paytan, A.; Price, N. N.; Peterson, B.; Takeshita, Y.; Matson, P. G.; Crook, E. D.; Kroeker, K. J.; Gambi, M. C.; Rivest, E. B.; Frieder, C. A.; Yu, P. C.; Martz, T. R. High-frequency dynamics of ocean pH: A multi-ecosystem comparison. *PLoS One* **2011**, *6*, No. e28983.

(26) Frieder, C. A.; Nam, S. H.; Martz, T. R.; Levin, L. A. High temporal and spatial variability of dissolved oxygen and pH in a nearshore California kelp forest. *Biogeosciences* **2012**, *9*, 3917−3930.

https://doi.org/10.1021/acs.est.2c00010
Environ. Sci. Technol. 2022, 56, 9015−9028

(27) Kapsenberg, L.; Cyronak, T. Ocean acidification refugia in variable environments. *Glob. Change Biol.* **2019**, *25*, 3201−3214.
(28) Cornwall, C. E.; Hepburn, C. D.; McGraw, C. M.; Currie, K. I.; Pilditch, C. A.; Hunter, K. A.; Boyd, P. W.; Hurd, C. L. Diurnal fluctuations in seawater pH influence the response of a calcifying macroalga to ocean acidification. *Proc. Roy. Soc. B Biol. Sci.* **2012**, *280*, No. 20132201.
(29) Mangan, S.; Urbina, M. A.; Findlay, H. S.; Wilson, R. W.; Lewis, C. Fluctuating seawater pH/p CO_2 regimes are more energetically expensive than static pH/p CO_2 levels in the mussel *Mytilus edulis*. *Proc. Roy. Soc. B Biol. Sci.* **2017**, *284*, No. 20171642.
(30) Kapsenberg, L.; Miglioli, A.; Bitter, M. C.; Tambutté, E.; Dumollard, R.; Gattuso, J.-P. Ocean pH fluctuations affect mussel larvae at key developmental transitions. *Proc. Roy. Soc. B* **2018**, *285*, No. 20182381.
(31) Onitsuka, T.; Takami, H.; Muraoka, D.; Matsumoto, Y.; Nakatsubo, A.; Kimura, R.; Ono, T.; Nojiri, Y. Effects of ocean acidification with pCO_2 diurnal fluctuations on survival and larval shell formation of Ezo abalone, Haliotis discus hannai. *Mar. Environ. Res.* **2018**, *134*, 28−36.
(32) Bednaršek, N.; Tarling, G. A.; Bakker, D. C.; Fielding, S.; Feely, R. A. Dissolution dominating calcification process in polar pteropods close to the point of aragonite undersaturation. *PLoS One* **2014**, *9*, No. e109183.
(33) Bednaršek, N.; Feely, R. A.; Tolimieri, N.; Hermann, A. J.; Siedlecki, S. A.; Waldbusser, G. G.; McElhany, P.; Alin, S. R.; Klinger, T.; Moore-Maley, B.; Pörtner, H. O. Exposure history determines pteropod vulnerability to ocean acidification along the US West Coast. *Sci. Rep.* **2017**, *7*, 4526.
(34) Bednaršek, N.; Feely, R. A.; Beck, M. W.; Alin, S. R.; Siedlecki, S. A.; Calosi, P.; Norton, E. L.; Saenger, C.; Štrus, J.; Greeley, D.; Nezlin, N. P.; Roethler, M.; Spicer, J. I. Exoskeleton dissolution with mechanoreceptor damage in larval Dungeness crab related to severity of present-day ocean acidification vertical gradients. *Sci. Total Environ.* **2020**, *716*, No. 136610.
(35) Lischka, S.; Büdenbender, J.; Boxhammer, T.; Riebesell, U. Impact of ocean acidification and elevated temperatures on early juveniles of the polar shelled pteropod *Limacina helicina*: mortality, shell degradation, and shell growth. *Biogeosciences* **2011**, *8*, 919−932.
(36) Waldbusser, G. G.; Steenson, R. A.; Green, M. A. Oyster shell dissolution rates in estuarine waters: effects of pH and shell legacy. *J. Shellfish Res.* **2011**, *30*, 659−669.
(37) Byrne, M.; Fitzer, S. The impact of environmental acidification on the microstructure and mechanical integrity of marine invertebrate skeletons. *Conserv. Physiol.* **2019**, *7*, No. coz062.
(38) Clark, M. S. Molecular mechanisms of biomineralization in marine invertebrates. *J. Exp. Biol.* **2020**, No. jeb206961.
(39) Byrne, M.; Lamare, M.; Winter, D.; Dworjanyn, S. A.; Uthicke, S. The stunting effect of a high CO_2 ocean on calcification and development in sea urchin larvae, a synthesis from the tropics to the poles. *Philos. Trans. Roy. Soc. B Biol. Sci.* **2013**, *368*, No. 20120439.
(40) Fitzer, S. C.; Cusack, M.; Phoenix, V. R.; Kamenos, N. A. Ocean acidification reduces the crystallographic control in juvenile mussel shells. *J. Struct. Biol.* **2014**, *188*, 39−45.
(41) Fitzer, S. C.; Zhu, W.; Tanner, K. E.; Phoenix, V. R.; Kamenos, N. A.; Cusack, M. Ocean acidification alters the material properties of *Mytilus edulis* shells. *J. Roy. Soc. Interface* **2015**, *12*, No. 20141227.
(42) Garilli, V.; Rodolfo-Metalpa, R.; Scuderi, D.; Brusca, L.; Parrinello, D.; Rastrick, S. P.; Foggo, A.; Twitchett, R. J.; Hall-Spencer, J. M.; Milazzo, M. Physiological advantages of dwarfing in surviving extinctions in high-CO_2 oceans. *Nat. Clim. Change* **2015**, *5*, 678−682.
(43) Pan, T.-C. F.; Applebaum, S. L.; Manahan, D. T. Experimental ocean acidification alters the allocation of metabolic energy. *Proc. Natl. Acad. Sci. U. S. A.* **2015**, *112*, 4696−4701.
(44) Liu, W.; Yu, Z.; Huang, X.; Shi, Y.; Lin, J.; Zhang, H.; Yi, X.; He, M. Effect of ocean acidification on growth, calcification, and gene expression in the pearl oyster, Pinctada fucata. *Mar. Environ. Res.* **2017**, *130*, 174−180.
(45) Zhao, X.; Guo, C.; Han, Y.; Che, Z.; Wang, Y.; Wang, X.; Chai, X.; Wu, H.; Liu, G. Ocean acidification decreases mussel byssal attachment strength and induces molecular byssal responses. *Mar. Ecol. Prog. Ser.* **2017**, *17*, 67−77.
(46) Sadler, D. E.; Lemasson, A. J.; Knights, A. M. The effects of elevated CO_2 on shell properties and susceptibility to predation in mussels *Mytilus edulis*. *Mar. Environ. Res.* **2018**, *139*, 162−168.
(47) Meng, Y.; Guo, Z.; Yao, H.; Yeung, K. W.; Thiyagarajan, V. Calcium carbonate unit realignment under acidification: A potential compensatory mechanism in an edible estuarine oyster. *Mar. Pollut. Bull.* **2019**, *139*, 141−149.
(48) Checa, A. G.; Rodríguez-Navarro, A. B.; Esteban-Delgado, F. J. The nature and formation of calcitic columnar prismatic shell layers in pteriomorphian bivalves. *Biomaterials* **2005**, *26*, 6404−6414.
(49) Lee, S. W.; Jang, Y. N.; Kim, J. C. Characteristics of the aragonitic layer in adult oyster shells, *Crassostrea gigas*: Structural study of myostracum including the adductor muscle scar. *Mar. Biotechnol.* **2011**, *2011*, No. 742963.
(50) Fitzer, S. C.; Torres Gabarda, S.; Daly, L.; Hughes, B.; Dove, M.; O'Connor, W.; Potts, J.; Scanes, P.; Byrne, M. Coastal acidification impacts on shell mineral structure of bivalve mollusks. *Ecol. Evol.* **2018**, *8*, 8973−8984.
(51) Carriker, M. R.; Palmer, R. E.; Prezant, R. S. Functional ultramorphology of the dissoconch valves of the oyster *Crassostrea virginica*. *Proc. Natl. Shellfish. Assoc.* **1980**, *70*, 139−183.
(52) Checa, A. G. Physical and biological determinants of the fabrication of molluscan shell microstructures. *Front. Mar. Sci.* **2018**, *5*, 353.
(53) Harper, E. M.; Checa, A. Physiological versus biological control in bivalve calcite prisms: Comparison of euheterodonts and pteriomorphs. *Biol. Bull.* **2017**, *232*, 19−29.
(54) FAO Fisheries & Aquaculture. *Cultured Aquatic Species Information Programme—Crassostrea gigas (Thunberg, 1793)*. Food and Agriculture Organization of the United Nations: Rome. Retrieved June 1, 2020 from https://www.fao.org/fishery/en/culturedspecies/Crassostrea_gigas/en
(55) Barton, A.; Hales, B.; Waldbusser, G. G.; Langdon, C.; Feely, R. A. The Pacific oyster, *Crassostrea gigas*, shows negative correlation to naturally elevated carbon dioxide levels: Implications for near-term ocean acidification effects. *Limnol. Oceanogr.* **2012**, *57*, 698−710.
(56) Barton, A.; Waldbusser, G. G.; Feely, R. A.; Weisberg, S. B.; Newton, J. A.; Hales, B.; Cudd, S.; Eudeline, B.; Langdon, C. J.; Jefferds, I.; King, T.; Suhrbier, A.; McLaughlin, K. Impacts of coastal acidification on the Pacific Northwest shellfish industry and adaptation strategies implemented in response. *Oceanography* **2015**, *25*, 146−159.
(57) Hettinger, A.; Sanford, E.; Hill, T. M.; Russell, A. D.; Sato, K. N.; Hoey, J.; Forsch, M.; Page, H. N.; Gaylord, B. Persistent carry-over effects of planktonic exposure to ocean acidification in the Olympia oyster. *Ecology* **2012**, *93*, 2758−2768.
(58) Hettinger, A.; Sanford, E.; Hill, T. M.; Lenz, E. A.; Russell, A. D.; Gaylord, B. Larval carry-over effects from ocean acidification persist in the natural environment. *Glob. Change Biol.* **2013**, *19*, 3317−3326.
(59) Waldbusser, G. G.; Hales, B.; Langdon, C. J.; Haley, B. A.; Schrader, P.; Brunner, E. L.; Gray, M. W.; Miller, C. A.; Gimenez, I. Saturation-state sensitivity of marine bivalve larvae to ocean acidification. *Nat. Clim. Change* **2015**, *5*, 273−280.
(60) Suchanek, T. Extreme biodiversity in the marine environment: Mussel bed communities of *Mytilus californianus*. *Northwest Environ. J.* **1992**, *8*, 150−152.
(61) Beck, M. W.; Brumbaugh, R. D.; Airoldi, L.; Carranza, A.; Coen, L. D.; Crawford, C.; Defeo, O.; Edgar, G. J.; Hancock, B.; Kay, M. C.; Lenihan, H. S.; Luckenbach, M. W.; Toropova, C. L.; Zhang, G.; Guo, X. Oyster reefs at risk and recommendations for conservation, restoration, and management. *BioScience* **2011**, *61*, 107−116.

https://doi.org/10.1021/acs.est.2c00010
Environ. Sci. Technol. 2022, 56, 9015−9028

(62) NOAA Fisheries. *Global Aquaculture (National)*. NOAA, 2019 (May 22). https://www.fisheries.noaa.gov/national/aquaculture/global-aquaculture
(63) NOAA Fisheries. *Fisheries of the United States, 2018 (Alaska, New England/Mid-Atlantic, Pacific Islands, Southeast, West Coast, National)*. NOAA, 2020 (February 21). https://www.fisheries.noaa.gov/trait-story/fisheries-united-states-2018
(64) Ruesink, J. L.; Lenihan, H. S.; Trimble, A. C.; Heiman, K. W.; Micheli, F.; Byers, J. E.; Kay, M. C. Introduction of non-native oysters: Ecosystem effects and restoration implications. *Annu. Rev. Ecol. Evol. Syst.* **2005**, *36*, 643−689.
(65) Smaal, A.; van Stralen, M.; Craeymeersch, J. Does the introduction of the Pacific oyster *Crassostrea gigas* lead to species shifts in the Wadden Sea? In *The Comparative Roles of Suspension-Feeders in Ecosystems*; Springer: Dordrecht, 2005; pp. 277−289.
(66) Herbert, R. J.; Humphreys, J.; Davies, C. J.; Roberts, C.; Fletcher, S.; Crowe, T. P. Ecological impacts of non-native Pacific oysters (*Crassostrea gigas*) and management measures for protected areas in Europe. *Biodivers. Conserv.* **2016**, *25*, 2835−2865.
(67) Grinsted, A.; Moore, J. C.; Jevrejeva, S. Application of the cross wavelet transform and wavelet coherence to geophysical time series. *Nonlinear Process Geophys.* **2014**, *11*, 561−566.
(68) Torrence, C.; Compo, G. P. A practical guide to wavelet analysis. *Bull. Am. Meteorol. Soc.* **1998**, *79*, 61−78.
(69) Helsel, D. R.; Hirsch, R. M.; Ryberg, K. R.; Archfield, S. A.; Gilrow, E. J. Techniques and methods, 4-A3. In *Statistical Methods in Water Resources*; U.S. Geological Survey, 2020
(70) Beniash, E.; Ivanina, A.; Lieb, N. S.; Kurochkin, I.; Sokolova, I. M. Elevated level of carbon dioxide affects metabolism and shell formation in oysters *Crassostrea virginica*. *Mar. Ecol. Prog. Ser.* **2010**, *419*, 95−108.
(71) Dickinson, G. H.; Ivanina, A. V.; Matoo, O. B.; Pörtner, H. O.; Lannig, G.; Bock, C.; Beniash, E.; Sokolova, I. M. Interactive effects of salinity and elevated CO_2 levels on juvenile eastern oysters, *Crassostrea virginica*. *J. Exp. Biol.* **2012**, *215*, 29−43.
(72) Chandra Rajan, K.; Meng, Y.; Yu, Z.; Roberts, S. B.; Vengatesen, T. Oyster biomineralization under ocean acidification: from genes to shell. *Glo. Change Biol.* **2021**, *27*, 3779−3797.
(73) Le Moullac, G.; Soyez, C.; Vidal-Dupiol, J.; Belliard, C.; Fievet, J.; Sham-Koua, M.; Lo-Yat, A.; Saulnier, D.; Gaertner-Mazouni, N.; Guéguen, Y. Impact of pCO_2 on the energy, reproduction and growth of the shell of the pearl oyster *Pinctada margaritifera*. *Estuar. Coast. Shelf Sci.* **2016**, *182*, 274−282.
(74) Bednaršek, N.; Johnson, J.; Feely, R. A. Comment on Peck et al.: Vulnerability of pteropod (*Limacina helicina*) to ocean acidification: Shell dissolution occurs despite an intact organic layer. *Deep Sea Res. Part II Top. Stud. Oceanogr.* **2016**, *127*, 53−56.
(75) Byrne, R. H.; Acker, J. G.; Betzer, P. R.; Feely, R. A.; Cates, M. H. Water column dissolution of aragonite in the Pacific Ocean. *Nature* **1984**, *312*, 321−326.
(76) Dauphin, Y.; Ball, A. D.; Castillo-Michel, H.; Chevallard, C.; Cuif, J.-P.; Farre, B.; Pouvreau, S.; Salomé, M. In situ distribution and characterization of the organic content of the oyster shell *Crassostrea gigas* (Mollusca, Bivalvia). *Micron.* **2013**, *44*, 373−383.
(77) Chadwick, M.; Harper, E. M.; Lemasson, A.; Spicer, J. I.; Peck, L. S. Quantifying susceptibility of marine invertebrate biocomposites to dissolution in reduced pH. *Roy. Soc. Open Sci.* **2019**, *6*, No. 190252.
(78) Grear, J.; Pimenta, A.; Booth, H.; Horowitz, D. B.; Mendoza, W.; Liebman, M. In situ recovery of bivalve shell characteristics after temporary exposure to elevated pCO_2. *Limnol. Oceanogr.* **2020**, *65*, 2337−2351.
(79) Sanford, E.; Gaylord, B.; Hettinger, A.; Lenz, E. A.; Meyer, K.; Hill, T. M. Ocean acidification increases the vulnerability of native oysters to predation by invasive snails. *Proc. Roy. Soc. B Biol. Sci.* **2014**, *281*, No. 20132681.
(80) Breitburg, D. L.; Miller, T. Are oyster reefs essential fish habitat? Use of oyster reefs by ecologically and commercially important species. *J. Shellfish Res.* **1998**, *17*, 1293.
(81) Watson, S.-A.; Southgate, P. C.; Tyler, P. A.; Peck, L. S. Early larval development of the Sydney rock oyster *Saccostrea glomerata* under near-future predictions of CO_2-driven ocean acidification. *J. Shellfish Res.* **2009**, *28*, 431−437.
(82) Timmins-Schiffman, E.; Coffey, W. D.; Hua, W.; Nunn, B. L.; Dickinson, G. H.; Roberts, S. B. Shotgun proteomics reveals physiological response to ocean acidification in *Crassostrea gigas*. *BMC Genom.* **2014**, *15*, 951.
(83) Bible, J. M.; Cheng, B. S.; Chang, A. L.; Ferner, M. C.; Wasson, K.; Zabin, C. J.; Latta, M.; Sanford, E.; Deck, A.; Grosholz, E. D. Timing of stressors alters interactive effects on a coastal foundation species. *Ecology* **2017**, *98*, 2468−2478.
(84) Kroeker, K. J.; Sanford, E.; Rose, J. M.; Blanchette, C. A.; Chan, F.; Chavez, F. P.; Gaylord, B.; Helmuth, B.; Hill, T. M.; Hofmann, G. E.; McManus, M. A.; Menge, B. A.; Nielsen, K. J.; Raimondi, P. T.; Russell, A. D.; Washburn, L. Interacting environmental mosaics drive geographic variation in mussel performance and predation vulnerability. *Ecol. Lett.* **2016**, *19*, 771−779.
(85) Hollarsmith, J. A.; Sadowski, J. S.; Picard, M. M.; Cheng, B.; Farlin, J.; Russell, A.; Grosholz, E. D. Effects of seasonal upwelling and runoff on water chemistry and growth and survival of native and commercial oysters. *Limnol. Oceanogr.* **2020**, *65*, 224−235.
(86) Unsworth, R. K.; Collier, C. J.; Henderson, G. M.; McKenzie, L. J. Tropical seagrass meadows modify seawater carbon chemistry: Implications for coral reefs impacted by ocean acidification. *Environ. Res. Lett.* **2012**, *7*, No. 024026.
(87) Sorte, C. J. B.; Bracken, M. E. S. Warming and elevated CO_2 interact to drive rapid shifts in marine community production. *PLoS One* **2015**, *10*, No. e0145191.
(88) Kapsenberg, L.; Hofmann, G. E. Ocean pH time-series and drivers of variability along the northern Channel Islands, California, USA. *Limnol. Oceanogr.* **2016**, *61*, 953−968.
(89) Kwiatkowski, L.; Gaylord, B.; Hill, T.; Hosfelt, J.; Kroeker, K. J.; Nebuchina, Y.; Ninokawa, A.; Russell, A. D.; Rivest, E. B.; Sesboüé, M.; Caldeira, K. Nighttime dissolution in a temperate coastal ocean ecosystem increases under acidification. *Sci. Rep.* **2016**, *6*, 22984.
(90) Hendriks, I. E.; Olsen, Y. S.; Ramajo, L.; Basso, L.; Steckbauer, A.; Moore, T. S.; Howard, J.; Duarte, C. M. Photosynthetic activity buffers ocean acidification in seagrass meadows. *Biogeosciences* **2014**, *11*, 333−346.
(91) Nielsen, K. J.; Stachowica, J. J.; Boyer, K.; Bracken, M.; Chan, F.; Chavez, F.; Hovel, K.; Kent, M.; Nickols, K.; Ruesink, J.; Tyburczy, J.; Wheeler, S. *Emerging Understanding of the Potential Role of Seagrass and Kelp as an Ocean Acidification Management Tool in California*; California Ocean Science Trust, 2018.
(92) Britton, D.; Cornwall, C. E.; Revill, A. T.; Hurd, C. L.; Johnson, C. R. Ocean acidification reverses the positive effects of seawater pH fluctuations on growth and photosynthesis of the habitat-forming kelp, *Ecklonia radiata*. *Sci. Rep.* **2016**, *6*, 26036.
(93) Wahl, M.; Covachã, S. S.; Saderne, V.; Hiebenthal, C.; Müller, J. D.; Pansch, C.; Sawall, Y. Macroalgae may mitigate ocean acidification effects on mussel calcification by increasing pH and its fluctuations. *Limnol. Oceanogr.* **2018**, *63*, 3−21.

https://doi.org/10.1021/acs.est.2c00010
Environ. Sci. Technol. 2022, 56, 9015−9028